Hα spectropolarimetry of B[e] and Herbig Be stars

René D. Oudmaijer & Janet E. Drew

Imperial College of Science, Technology and Medicine, Blackett Laboratory, Prince Consort Road,
London, SW7 2BZ, U.K.

arXiv:astro-ph/9901032v1 5 Jan 1999

ABSTRACT

We present the results of medium resolution ($\Delta v \approx 60 \, \mathrm{km \, s^{-1}}$) spectropolarimetric observations across Hα of a sample of B[e] and Herbig Be objects. A change in linear polarization across Hα is detected in a large fraction of the objects, with characteristics ranging from simple depolarization in a couple of Herbig Be stars, to more complex behaviour in the probable post main sequence B[e] stars. Hα in the spectra of HD 37806 and HD 50138 each consist of a double-peaked polarized line and a superposed unpolarized single emission peak, suggesting two distinct line-forming regions. Multiple observations of HD 45677 allow for the separation of electron and dust scattering effects for the first time: the difference between derived intrinsic polarization angles of the two components indicate that the dust-scattering region is clumpy. Two unexpected results are the non-detections of Hα polarization changes in ω Ori, where depolarization has previously been detected, and in MWC 297, which exhibits source elongation at radio wavelengths. In ω Ori time variability is probably responsible such that this star's electron-scattering disk was much weakened at the time of observation. Two hypotheses are advanced that might explain the MWC 297 result.

The general findings are that roughly half of the observed Herbig Be stars show polarization changes across Hα, implying immediately that their ionized envelopes are not spherically symmetric. This pattern, if confirmed by observations of a larger sample, could indicate that the non-detection rate is simply a consequence of sampling randomly-oriented circumstellar disks able to scatter starlight within a few stellar radii. The stars classified as B[e] stars all show startling polarization changes across Hα. The details in each case are different, but the widely accepted concept of dense Hα-emitting equatorial disks around these objects is supported.

Key words: stars: circumstellar matter – stars: pre-main sequence – stars: emission line, Be – stars: mass loss – polarization

1 INTRODUCTION

Classification of a star as a Be star has long been recognised as consignment to a loosely defined phenomenological group, rather than as a definition of the evolutionary status of the star. Presently the Be stars may be divided into three main groups: (i) the classical Be stars, generally thought of as the most rapidly rotating near main sequence B stars (see e.g. Slettebak, 1988); (ii) the Herbig Be stars, first identified by Herbig (1960) as stars in the B spectral type range whose association with star-forming regions and emission line character might indicate that they are very young; (iii) the B[e] stars (Allen & Swings, 1976; Zickgraf et al. 1985), noted for the presence of forbidden line as well as HI emission in their spectra and strong IR continuum excesses (also seen in Herbig Be stars). While it was initially thought that B[e] stars are preferentially supergiants, recent work (Gummersbach

et al. 1995) has demonstrated from deep LMC observations that B[e] characteristics may also be seen at significantly lower luminosities.

It is now widely accepted that classical Be stars are encircled at their equators by ionized, low opening angle, almost Keplerian, disks, that are optically-thick in Hα. By contrast, the circumstellar geometry of Herbig Be and B[e] stars is rather more of an open question. In this work, we will open up another avenue for exploring this issue. We present medium resolution spectropolarimetry across the Hα line, a technique that, in the case of the detection of polarization changes across the line can provide an answer to the most basic question "Is the ionized material around these stars spherically symmetric or not?".

By comparing Hα polarization with that of the continuum one can exploit the fact that line and continuum respec-

tively form within a larger and smaller volume and subsequently 'see' different scattering geometries. Essentially, Hα is not significantly scattered by the ionized envelope in which it forms, whereas the continuum arising primarily from the central star embedded in the envelope undergoes electron scattering. In the case that the ionized envelope's projection on to the plane of the sky is non-circular, a net linear polarization is imprinted on the continuum light, but not on Hα producing a drop in the polarization percentage across the line ('line-effect'). The addition of further continuum polarization by either a dusty envelope or the ISM modifies this change and may even produce a net percentage rise across the line – but, significantly, it cannot nullify the change. For example, Schulte-Ladbeck et al. (1994) showed that the Hα emission line of AG Car displayed enhanced polarization at one epoch while on other occasions a de-polarization across the line was observed. After the correction for ISP however, Hα was de-polarized with respect to the continuum on all occasions.

The advantage of spectropolarimetry over broadband polarimetry is that a result can be obtained even where it is not possible to distinguish the various contributions to the total continuum polarization. Furthermore, by spectrally-resolving the Hα line profile one can hope to pick out more subtle effects arising in cases where the assumption that the Hα emission is unscattered, and hence unpolarized, breaks down. Qualitatively these were demonstrated in model calculations by Wood, Brown & Fox (1993). When there is significant scattering of Hα the line profile in linear polarized light becomes a probe of the velocity field in the electron-scattering medium. Using this tool we have already shown in the case of the B[e] star, HD 87643, that there is direct evidence of a rotating and expanding outflow (Oudmaijer et al 1998).

The pioneering work in this area was made in the seventies, when Clarke & McLean (1974), Poeckert (1975) and Poeckert & Marlborough (1976, hereafter PM) conducted narrow-band polarimetric studies of Be stars that compared the linear polarization on and off Hα. Many instances of line de-polarization were found, showing that the envelopes of Be stars do not project as circles onto the sky. After this time, polarimetric studies were made of several classes of object, but due to observational difficulties it remained a specialist activity. However in the past few years there has been rising interest in the technique. Spectropolarimetry has been performed on several strong Hα emitting evolved stars, such as AG Car and HR Car (Schulte-Ladbeck et al. 1994, Clampin et al. 1995), where the position angle of the spatially-unresolved flattened electron scattering region has been shown to agree with the observed extension of the optically visible nebulae surrounding these objects. Both the B[e] and Herbig Be stars are ideal objects to subject to this style of observation, since they are strong Hα emitters and often optically bright enough to render studies at medium resolution with high photon counts feasible with 4-meter class telescopes. Furthermore there is a clear need for this type of observation since a change in the linear polarization across Hα can be the only direct evidence of electron scattering operating on the scale of a few stellar radii as opposed to polarization by a dusty envelope.

In the first instance, the observations presented here were motivated by the aim of examining Herbig Be stars for the presence of ionized circumstellar disks. These reputedly intermediate mass objects present a phenomenology that suggests they are approaching or have recently achieved a main sequence location on the HR diagram – they are the higher mass counterparts of the T Tauri stars. The paradigm for star formation invokes a collapsing cloud and conservation of angular momentum that results in the formation of a flattened circumstellar (accretion) disk, that eventually accretes or is blown away by an outflow. However there is not yet a consensus that accretion disks are commonly associated with the known Herbig Be (and Ae) stars. There is a certain irony that T Tauri stars, their lower mass counterparts, are generally accepted to have disk-like envelopes (e.g. HH30 in Burrows et al. 1996), while evidence is accumulating that their higher mass counterparts, the optically obscured massive Young Stellar Objects (YSOs) are also surrounded by disk-like structures (e.g. Hoare & Garrington 1995, and references therein).

MERLIN radio data on MWC 297, a nearby radio-bright early Herbig Be star, also reveals an elongated (but ionized) structure on a spatial scale of $\sim$100 AU (Drew et al. 1997). More direct high resolution imaging is clearly worthwhile and of course spectropolarimetry can help identify interesting targets. Nevertheless, at the present, there persists a debate that the observed spectral energy distributions require, on the one hand, dusty disks (e.g. Malfait, Bogaert & Waelkens, 1998) or, on the other, that they can be fit satisfactorily by spherically symmetric dusty envelopes (Miroshnichenko, Ivezić & Elitzur, 1997; see also the overview of this issue in Pezzuto, Strafella & Lorenzetti 1997). The recent direct detection of a rotating disk around a Herbig Ae star by Mannings, Koerner & Sargent (1997) indicates that at least some of these objects have disk-like geometries. Broad-band polarimetry of a number of Herbig stars has revealed variability of the polarization of the objects which could imply deviations from spherical symmetry of the dusty envelopes (e.g. Grinin et al. 1994, who studied UX Ori; Jain & Bhatt, 1995). By contrast, the Hα spectropolarimetry traces scales even closer to the star, the ionized material.

With regard to the B[e] stars, first picked out by Allen & Swings (1976), the argument for embedding them in disk-like equatorial structures has largely been won in that there is widespread acceptance of Zickgraf's phenomenological model (Zickgraf et al 1985, 1986). This is because there is compelling spectral evidence of a fast, presumably polar, wind at UV wavelengths, that combines with a high emission measure, much more slowly expanding, presumably equatorial, flow traced by strong optical emission lines. Broad-band polarimetry by Zickgraf & Schulte-Ladbeck (1989) and Magalhães (1992) indicate that for a sub-sample of B[e] objects, the circumstellar dust, located at larger distances from the star, is distributed in a geometry deviating from spherically symmetric. The unresolved issue is how these axially-symmetric structures arise and indeed what the stellar evolutionary status of this object class really is. The fact that B[e] stars are far from being exclusively supergiants deepens the mystery. In this context, Herbig's (1994) concern about the difficulty of distinguishing Herbig Be from B[e] stars becomes all the more intriguing. To progress in understanding how B[e] disks arise, a more complete description of the disk density and velocity field is highly desirable. It is

in this respect that Hα spectropolarimetry has the potential to provide unique insights.

Because of the problems of distinguishing between the B[e] and Herbig Be categories, there is always a significant probability that a Herbig Be sample contains some B[e] stars. Indeed, for Galactic B[e] stars it is often difficult to determine whether an object is a luminous evolved object or a less luminous pre-main sequence object (see e.g. the discussions on HD 87643; Oudmaijer et al.1998, MWC 137; Esteban & Fernández 1998, and HD 45677; de Winter & van den Ancker 1997). Here we exploit this in that our programme of Hα spectropolarimetry programme includes as targets relatively clear-cut examples of post main sequence B[e] stars alongside undisputed Herbig Be stars and objects that might be either. In this paper we give an overview of our observing campaign to date. In Section 2, the way in which targets were selected and the observations are discussed. The results and their interpretation are presented on a case-by-case basis in Sec. 3. Sec. 4 contains a discussion on the power of spectropolarimetry and what we have learned from this program. We conclude in Sec. 5.

2 OBSERVATIONS

2.1 Sample selection

The target stars were selected from the catalogue of Thé, de Winter & Perez (1994) which lists all objects that had been at that time proposed to be Herbig Ae/Be objects, and provides tables of other emission type objects whose nature is not clear. The list of targets is provided in Table 1. The targets were not selected with foreknowledge of envelope asphericity, rather, they were chosen because of their relative brightness, their position on the sky, and their early (B-type) spectral types.

2.2 Spectropolarimetry

The optical linear spectropolarimetric data were obtained using the RGO Spectrograph with the 25cm camera on the 3.9-metre Anglo-Australian telescope during three observing runs in January 1995, December 1995 and December 1996 respectively. During the first two runs, the weather provided some spectacular views of lightning from the telescope, but only limited data. During clear time, we aimed at observing the brightest objects in order to make the best of lower-than-desired count rates. Nevertheless, the resulting polarization measurements proved to be very stable. The last run was mostly clear, opening the way for time to be spent on some of our fainter targets.

The instrumental set-up was similar during all observing runs and consisted of a rotating half-wave plate and a calcite block to separate the light into perpendicularly polarized light waves. Two holes of size 2.7 arcsec and separated by 22.8 arcsec in the dekker allow simultaneous observations of the object and the sky. Four spectra are recorded, the O and E rays of the target object and the sky respectively. One complete polarization observation consists of a series of consecutive exposures at four rotator positions. Per object, several cycles of observation at the four rotator positions were obtained in order to check on the repeatability of the

results. Indeed, we find that multiple observations of the same star result in essentially the same polarization spectrum. To prevent the CCD from saturating on the peak of Hα, shorter integration times were adopted for those objects with particularly strong Hα emission. Spectropolarimetric and zero-polarization standards were observed every night.

A 1024 × 1024 pixel TEK-CCD detector was used which, combined with the 1200V grating, yielded a spectral range of 400 Å, centered on Hα. Wavelength calibration was performed by observing a copper-argon lamp before or after each object was observed. In all observations reported here a slit width of 1.5″ was used. A log of the observations is provided in Table 1. Bias-subtraction, flatfielding, extraction of the spectra and wavelength calibration was performed in IRAF (Tody 1993). The resulting spectral resolution as measured from arc lines is 60 km s⁻¹. The E and O ray data were then extracted and imported into the Time Series/Polarimetry Package (TSP) incorporated in the FIGARO software package maintained by STARLINK. The Stokes parameters were determined and subsequently extracted.

A slight drift of a few degrees in position angle (PA) was calibrated by fitting its wavelength dependence in nightly 100% polarized observations of bright unpolarized stars (obtained by inserting an HN-22 filter in the light-path) and removed from the polarization spectra. The instrumental polarization deduced from observations of unpolarized standards proved to be smaller than 0.1% in all cases.

In July 1998, MWC 297 was observed in service time with the ISIS spectrograph and polarimetric optics on the 4.2m William Herschel Telescope, La Palma. The instrumental set-up included the 1200R grating and a 1124×1124 TEK2 detector, providing a wavelength coverage of 400 Å around Hα and a spectral resolution of 40 km s⁻¹. The data reduction was the same as for the AAT data.

Polarization accuracy is in principle only limited by photon-statistics. One roughly needs to detect 1 million photons per resolution element to achieve an accuracy of 0.1% in polarization (the fractional error goes at $\sim 1/\sqrt{N}$). However, although it is probably fair to say that the internal consistency of a polarization spectrum follows photon-statistics, the external consistency (i.e. the absolute value for the polarization, checking for variability) is limited due to systematic errors. For example, when calculating the polarization of a given spectral interval one can reach polarization percentages with a statistical error of several thousandth of a percent. However, instrumental polarization (less than 0.1%), scattered light and low-level intrinsic variability of the polarization standards may influence the zero-points. The quality and amount of data taken of spectropolarimetric standard stars is at present not yet sufficient to reach absolute accuracies below the 0.1% mark (see manual by Tinbergen & Rutten, 1997). A feeling for the possible accuracies in our data can be obtained by studying some of the objects that have been observed on different occasions. Seven, respectively 6 independent observations of the Be star HD 76534 and the polarization standard HD 80558 yield a mean polarization and rotation of (0.49 % with an r.m.s. scatter of 0.03 %, 124° with a scatter of 3°) and (3.19 ± 0.11% , 162 ± 1.6°) respectively. It is encouraging to note that our independent continuum measurements stretching over more than a year are mostly within 0.1%, and often within 0.05%, in polarization.

Table 1. Targets

Name	Other name	V	Spectral Type	Date	Integration (s)
HD 37806	MWC 120	8.0	B9Ve+sh	11-01-95	4×120
				31-12-96	16×90
ω Ori	HD 37490	4.6	B3III/IVe	11-01-95	8×15
V380 Ori	BD-06 1253	10.0	B8/A1e	31-12-96	12×300
MWC 137	PK 195-00.1	11.2	B0ep	31-12-96	16×200, 8×300
HD 259431	MWC 147	8.7	B5Vep	30-12-96	4×240, 8×180
HD 45677	FS CMa	7.6	B3[e]p+sh	11-01-95	24×20
				30-12-96	32×10
HD 50138	MWC 158	6.7	B6V[e]+sh	11-01-95	16×30
				01-01-97	24×60
AS 116	BD-10 1351	9.6	Be	01-01-97	32×300
HD 53367	MWC 166	6.9	B0III/IVe	30-12-96	8×90
				01-01-97	8×240
LkHα 218		11.9	B6e	31-12-96	20×300
HD 52721	GU CMa	6.6	B2Vne	11-01-95	8×100
HD 76534	He 3-225	8.0	B2/3ne	11-01-95	8×300
				31-12-95	4× 300
				30-12-96	4× 90, 4×180
				31-12-96	4× 90
He 3-230	PK 266-00.1	-	Be	30-12-96	24×300
HD 87643	He 3-365	8.5	B3/4[e]	31-12-96	20× 90
				01-01-97	12×120
MWC 297		12.3	B1.5Ve	15-07-98	56×100

Spectral types taken from Thé et al. (1994), except for MWC 297, taken from Drew et al. (1997). *V* magnitudes taken from SIMBAD.
The integration times denote the *total* on-source exposures.

Table 2. Results

Object	Date	Hα EW (Å)	line/cont	P_{cont} (%)	Θ_{cont} (°)	Line-effect?
HD 37806	Jan 95	−17	4.9	0.29 (0.01)	121 (1)	√
	Dec 96	−22	4.8	0.36 (0.01)	125 (1)	√
ω Ori		−3.5	1.6	0.30 (0.01)	55 (1)	-
V380 Ori		−79	14	1.26 (0.01)	96 (1)	-
MWC 137		−550	83	6.11 (0.01)	162 (1)	√
HD 259431		−63	11	1.06 (0.01)	102 (1)	√?
HD 53367		−14	2.6	0.49 (0.01)	44 (1)	√
HD 45677	Jan 95	−200	35	0.33 (0.01)	11 (1)	√
	Dec 96	−200	34	0.14 (0.02)	143 (3)	√
HD 50138	Jan 95	−67	13	0.71 (0.01)	161 (1)	√
	Dec 96	−58	13	0.65 (0.01)	154 (1)	√
AS 116		−90	18	1.41 (0.01)	30 (1)	-
LK Hα 218		−20	6	1.91 (0.02)	19 (1)	-?
HD 52721		−14	3	1.15 (0.01)	19.0 (1)	-
HD 76534	Jan 95	−7.5	2.0	0.52 (0.01)	124 (1)	-
	Dec 95	−4.0	1.8	0.49 (0.03)	122 (2)	-
	30 Dec 96	−6.1	1.9	0.50 (0.01)	125 (1)	-
	31 Dec 96	−3.7	1.7	0.47 (0.02)	128 (1)	-
Hen 3-230		−315	64	1.61 (0.02)	30 (1)	-
HD 87643	Dec 96	−186	25	0.84 (0.01)	168 (1)	√
	Jan 97	−196	26	0.75 (0.01)	164 (1)	√
MWC 297		−520	100	1.90 (0.01)	86 (1)	-

Continuum defined from 6400-6500 and 6600-6700 Å. The errors on the equivalent widths of the Hα lines are expected to be of order
5%, the errors cited for the polarization data are based on photon-statistics only, and rounded upwards. Systematic (i.e. external)
errors in the polarization are estimated to be of order 0.05% − 0.1%.

3 RESULTS

Some Hα parameters and continuum polarizations are presented in Table 2. In the following, the results across the full range of targets observed are summarized. These are grouped such that we begin with those objects showing no discernable polarization changes across Hα (§3.1), and then move on to objects which do show percentage changes and/or rotations (§3.2).

Unless specifically stated, we have made no attempt below to correct for the interstellar polarization (ISP). This decision is based on the following: the main goal of this study is the detection of polarimetric changes across the Hα line. Since the wavelength dependence of the interstellar polarization only becomes apparent on wavelength ranges larger than our spectra provide, the ISP will only contribute a constant polarization vector in (Q,U) space to the observed spectra. A further reason to refrain from ISP corrections here, is that the methods commonly used for this (field-star method and continuum variability, see e.g. McLean & Clarke 1979) do not always return unambiguous values. However, in the absence of ISP correction, it is useful to remember the point raised in the introduction that the ISP can change what might otherwise be a reduction of the linear polarization percentage across the Hα line into an increase in polarization, or an apparently constant polarization, but accompanied by a significant rotation in the position angle. The same effect can occur in the event of additional polarization due to circumstellar dust.

Nevertheless, regardless of the influence of the ISP and polarization due to circumstellar dust, it is possible to derive the *intrinsic* angle of the electron-scattering material (e.g. Schulte-Ladbeck et al.1994). Assuming the line is depolarized, the vector connecting the line- and continuum polarization in the QU plane will have a slope that is equivalent to the intrinsic angle of the scattering material responsible for the continuum polarization. Since the wavelength dependence of both circumstellar dust polarization and ISP is small, they add only a constant QU vector to all points in both line and continuum, and thus will not affect the difference in line-to-continuum polarization. This slope is measured as $\Theta = 0.5 \times \mathrm{atan}(\Delta U / \Delta Q)$.

3.1 Stars showing no clear change across Hα

In this subsection we discuss the objects that do not show a line-effect. In principle such an observation implies that the projection of the ionized region on the plane of the sky is (mostly) circular. We will find that this does not necessarily have to be the case. The objects falling into this group are Lk Hα 218, Hen 3-230, AS 116, HD 52721, V380 Ori, HD 76534, ω Ori and MWC 297. Their polarization spectra are shown in Figure 1.

Hen 3-230, AS 116, Lk Hα 218 These objects are relatively faint targets for which the signal-to-noise ratios in our data are not so high. Hence, the absence of change across Hα for the time being should be viewed as an absence of any marked contrast. For example in the case of Lk Hα 218, there seems enhanced polarization at the position of the stronger redshifted emission component in the line. However this is not strictly even a 2σ detection. Coarser binning can yield

a 3σ enhanced polarization in the line (at smaller resolution this is only present in one pixel however) but in truth it would appear that 100 minutes exposure is not enough for this object. The null results for Hen 3-230 and AS 116 are more sure. Both targets have extremely bright line emission. As previous observations of them are extremely sparse, their evolutionary status remains undetermined. Based on its low excitation spectrum Stenholm & Acker (1987) argue that Hen 3-230 is not a Planetary Nebula, despite having figured in many previous papers to be one. AS 116 was appeared in a catalogue of emission line stars of Miller & Merrill (1951), since then not much work has been published. The IRAS flux peaks at 25μm, which could point at a detached dust shell, but it was not detected in the OH maser by Blommaert, van der Veen & Habing (1993).

HD 52721, V380 Ori These are two quite convincing examples of no line effect. Both, nevertheless, present significant continuum polarizations. Since HD 52721 presents little of an infared continuum excess (Hillenbrand et al. 1992), it might seem plausible that this star is a low-inclination classical Be star behind a significant interstellar column. Indeed the single-peaked Hα emission is consistent with this, but in contrast to the $v \sin i$ measurement of 400±40 km s^{-1} reported by Finkenzeller (1985) suggesting high inclination. V380 Ori exhibiting a strong infrared continuum excess, would appear to be optically-veiled and hence sits more convincingly in the HAeBe object class. The absence of a line-effect in V380 Ori may simply imply lower inclination to the line of sight.

HD 76534 The initial 1995 data on this source have already been presented by Oudmaijer & Drew (1997). There it was shown that these data did not indicate any changes across Hα. Our new data confirm this and show no hints of pronounced polarization variability in its modest ∼0.5% level. This is despite the source's propensity for spectral variability clearly illustrated by the 11 January 1995 transformation of Hα absorption into well-developed double-peaked emission within hours (Oudmaijer & Drew 1997). Table 2 lists the Hα equivalent widths at the various occasions that the object was observed. The EW changes strongly, but situations similar to the January 1995 data were not observed.

ω Ori It is not clear whether ω Ori should be considered a Herbig Be star, or simply a classical Be star (Sonneborn et al. 1988). The absence of a detectable change across Hα (Fig. 1) stands in contrast to reports in the literature that the hydrogen recombination lines show de-polarization – PM find that Hα shows a polarization dip while Clarke & Brooks (1984) find the same in Hβ. This difference is presumably connected with the stronger Hα emission reported by PM (line to continuum ratio of 1.8 versus our figure of 1.4 - which was not binned to the same narrow band, and is thus a strong upper limit), and higher linear polarization (0.38% versus our 0.30%). Since classical Be stars and, indeed, Herbig Be stars are known to be emission line variables, this change is probably due to a lowering of the ionized emission measure of the equatorial disk around this star. Given the great disparity between the Thomson scattering and Hα absorption cross-sections, a relatively modest drop in the Hα equivalent width could well be accompanied by a collapse
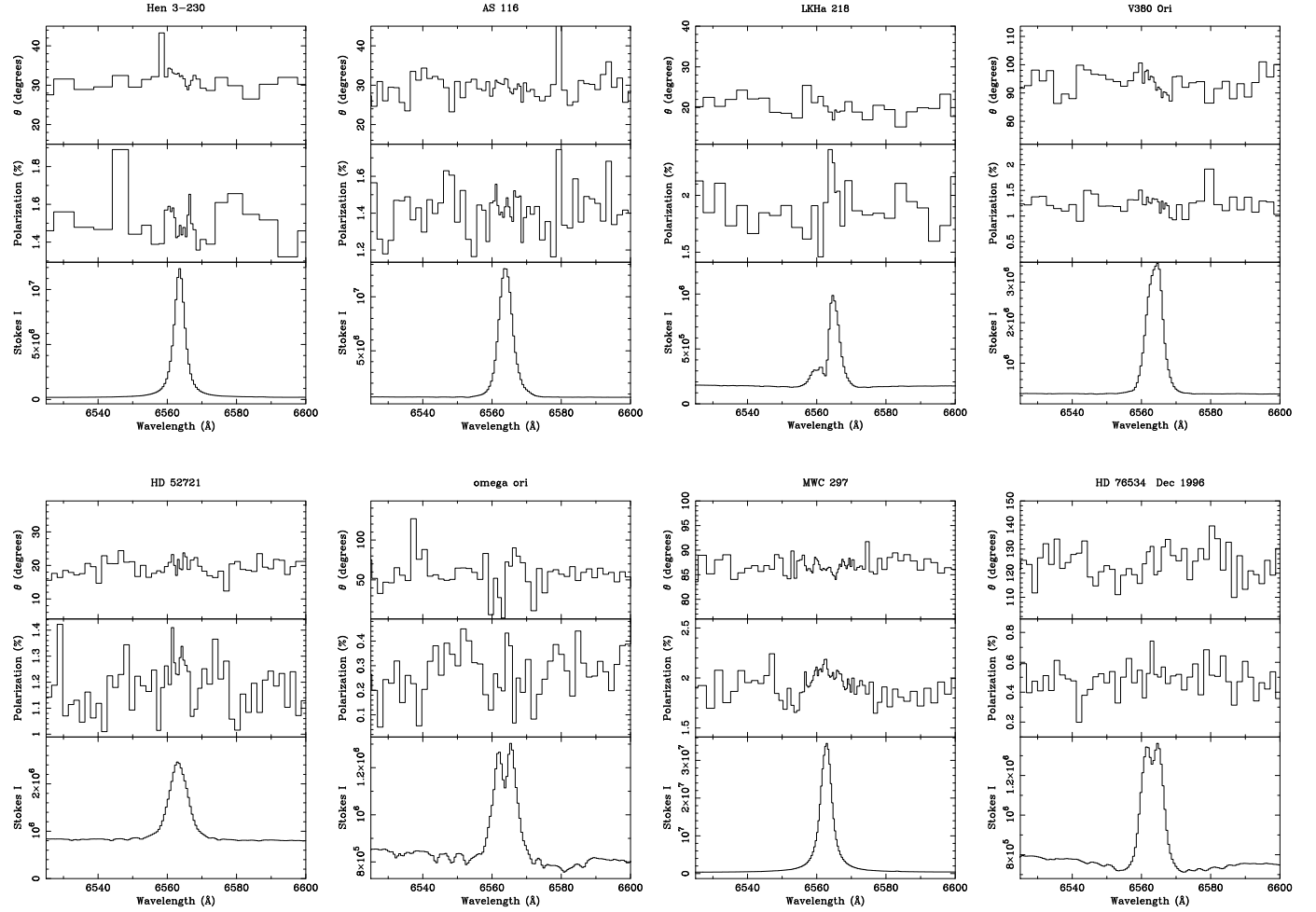
Figure 1. Polarization spectra of the stars showing no clear polarization change across Hα. In each case, the normal (intensity) spectrum is shown in the lower panel, the polarization (in %) in the middle panel, while the position angle is plotted in the upper panel. In each case and in the following figures (unless stated otherwise) the data are rebinned such that the 1σ error in the polarization corresponds to 0.1% as calculated from photon statistics.

in the percentage of linearly-polarized scattered starlight. Hence it would seem that ISP contributes around 0.3% linear polarization in ω Ori, a figure not out of line with PM's estimate of 0.24% .

MWC 297 The weak-to-non-existent effect across Hα is startling in view of the evidence gathered by Drew et al. (1997) that this early Herbig Be star is viewed at relatively high inclination. Furthermore, the 5 GHz radio image (see Drew et al. 1997), which provides an extinction-free view of the ionized circumstellar medium around MWC 297, indicates an elongated geometry that would suggest a line effect ought to be apparent in such a bright emission line source.

Although at first sight very surprising, we consider two different hypotheses that may explain this apparent paradox. Firstly, we can conclude we are seeing the Hα line directly, and that the line-forming region is indeed round. Since the Hα line is formed in a potentially much smaller volume than the continuum 5 GHz radiation, the rounder appearance of the Hα line-forming region indicates that the geometry changes between the near-stellar scale and the larger

scale sampled at radio wavelengths. Spatial evolution of this type has been predicted for lower mass stars (see Frank & Mellema 1996).

Secondly, it may be that Hα is formed in an edge-on disk like structure, but that the optical light does not reach us directly, and is completely obscured in the line-of-sight. The light that we see could then be 'mirrored' by scattering dust clouds located above and/or beneath the obscuring material. If the scattering dust-clouds 'see' a nearly circularly symmetric Hα emitting region, it will not see any depolarization across the line either. Consequently, the light reaching us will not show any polarization changes across Hα. That dust-scattering plays a role in this object is already suggested by the spectral energy distribution, which shows a notable excess in the U-band (Bergner et al. 1988; Hillenbrand et al 1992), possibly due to the 'blueing' effect.

We may therefore have a similar situation to that in the Red Rectangle (see e.g. Osterbart, Langer & Weigelt 1997, Waelkens et al 1996), where it was only recently realized that the central star is actually not the star itself, but its reflection against dusty knots located above and below a

very optically thick dust lane. This finding explained the long-standing problem of the energy balance; the apparently absorbed light from a star with such a modest reddening (A_V of order 1) is orders of magnitude less than that being re-radiated in the infrared.

If the circumstances are similar in MWC 297, the reddening ($A_V \approx 8$ - see discussion of Drew et al, 1997) commonly assigned to this source on the basis of conventional extinction measurements is a severe underestimate. This would not be completely unexpected, as MWC 297 is in certain respects an intermediate object between the optically visible Herbig Be stars, and their more massive counterparts, the Becklin-Neugebauer (BN) type objects, which suffer from large optical extinctions (A_V often in excess of 20). While in the optical, MWC 297 has much in common with the Herbig Be stars, at infrared and radio wavelengths it shows evidence of substantial mass loss associated with BN-type objects (Drew et al. 1997).

3.2 Objects displaying line effects

Here we present the objects for which the line-effect is observed. First, the Herbig Be stars in this sample are discussed, HD 259431, HD 53367 and HD 37806, then MWC 137, a Herbig Be star that has been recently proposed to be a massive evolved B[e] star instead is shown, and we end with the well-known B[e] objects HD 50138, HD 87643 and HD 45677.

HD 259431 We start with the least certain detection, HD 259431. This object (Fig. 2) shows a hint of de-polarization across Hα, from (1.1%, 102°) to 0.8% in the line center. The intrinsic polarization angle in QU space measured from the change from the continuum to line polarization, $\Theta = 0.5 \times \mathrm{atan}(\Delta U/\Delta Q)$, gives 17°, but with a large uncertainty. The length of this vector is small, of order 0.3%. Our two observations, taken one year apart, do not show any variability within the small error-bars. The compilation by Jain & Bhatt (1996) which contains broad-band polarimetric observations only hints at a slight variability. The high resolution data, only when binned to errors of 0.1% or less, show the line-effect.

HD 53367 The polarization spectrum of HD 53367 is shown in Fig. 2. Since there was no difference within the errorbars of the data taken on 2 consecutive nights, these were added to increase the signal-to-noise ratio. The Hα line is clearly de-polarized with respect to the continuum, while no rotation across the line is present. The intrinsic polarization angle in QU space measured from the slope is 47°.

If the line center is assumed to be completely de-polarized, one can use this information to correct the observed polarization for the ISP (the 'emission line method'). Reading off the polarization in the line-center (Q = 0.0%, U = 0.3%), and subtracting this value from the spectrum then gives an intrinsic polarization of 0.2 ± 0.01 % and a position angle of 44.5 ± 0.5° (measured in the bins 6400 – 6500 Å and 6700 – 6800 Å. Note that the error-bar reflects the internal consistency and not the external consistency), consistent with the slope in the QU plane. This low value of intrinsic continuum polarization is what one would expect from modest electron-scattering (see e.g. PM).
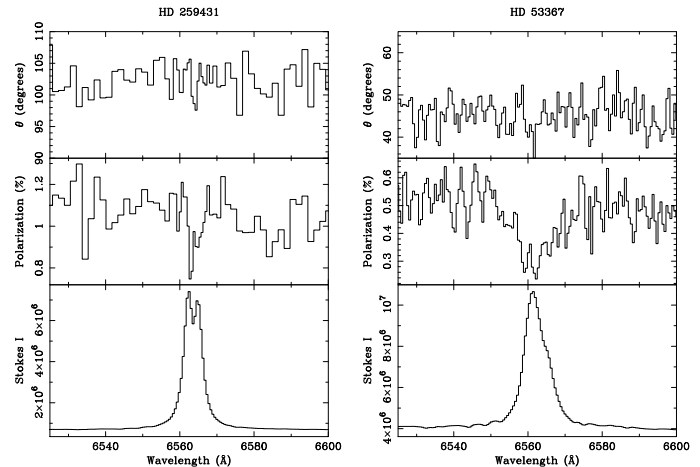

Figure 2. The polarization spectra of HD 259543 and HD 53367.

Let us now comment on the significance of the measured polarization angle. On the sky, HD 53367 is located on the periphery of the Canis Majoris 'hole' noted for its low reddening sightlines (Welsh 1991). Herbst, Racine & Warner (1978) designated this star a member of the CMa R1 cluster, which they placed at a distance of 1150 pc, the same distance as to the CMa OB1 association (Claria 1974). This distance is suspect as it makes HD 53367 more luminous than a supergiant at the same B0 spectral type. A more reasonable distance estimate would be around 550 pc (adopting a dereddened V magnitude of ~ 4; Herbst et al. 1982, and $M_V \simeq -4.7$; for a B0IV star, Schmidt-Kaler 1982). It is then less surprising that the Hipparcos catalogue (ESA, 1997) contains a finite, although very uncertain, parallax measurement for this star (see also van den Ancker, de Winter & Tjin A Djie 1998). In any event there is strong evidence that the cumulative interstellar extinction towards CMa R1 is not more than $A_V \simeq 0.2$, implying that the remaining observed extinction is local (Herbst et al. 1982; Vrba, Baierlein & Herbst 1987).

More important, Vrba et al. (1987) demonstrate quite convincingly that within CMa R1 the polarization angle tends to follow the sweep of the southern dust arc up through Sh2 292, the HII region ionized by HD 53367, and that the polarization is most likely due to grain alignment. At HD 53367 this angle is about 40° and entirely comparable to that of the non-emission line B3V star BD -10°1839 just $\sim$20 arcmin away, and also at a photometric distance of about 600 pc. The interesting feature of HD 53367 is that the separable intrinsic and foreground polarization angles are the same – as indicated by the lack of rotation across Hα in the observed spectrum. This suggests an orderly star formation process in which the rotation axis of HD 53367 'remembers' the larger scale circumstellar field direction, in preference to a more dynamical mechanism such as the 'accretion induced collision' merger model of Bonnell et al (1998), which would result in randomly oriented polarization angles.

HD 37806 The double peaked Hα profile of this object is remarkably different during our two observing epochs (Fig. 3). In December 1996, both peaks were equally bright, while in January 1995 the blue peak is much weaker. Although the signal-to-noise of the January 1995 data is not high, it appears that the object does not show significant changes in polarization. But a rotation is present, which is especially visible in the December 1996 data when the source was observed for longer. The rotation almost exactly occurs in the central dip in Hα, rather than across the entire adequately-resolved line profile. The fact that we observe only rotation is interesting in its own right, as the principle of line de-polarization without superimposed foreground polarization would imply a constant angle across Hα. Clearly there is ISP and perhaps circumstellar polarization present.

If we assume that the underlying, rotated part, of the line-profile is unpolarized, we may attempt a correction for the intervening interstellar- and circumstellar dust polarization, to retrieve the intrinsic spectrum of this object. The (Q,U) vector measured in the central dip of the rotation, corresponds to (-0.06%,0.35%) or a polarization of 0.36% with PA 50°. Subtracting these values from the observed spectra results in Fig.4. This figure also shows the 'polarized flux' (polarization × intensity). The polarized flux indicates that the double-peaked Hα line has the same polarization as the continuum, but – by virtue of the manner in which the ISP was corrected for – the central dip between the peaks is depolarized. The 1995 spectrum shows the same behaviour. Despite its much lower signal-to-noise, the large Red/Blue ratio has virtually disappeared in the polarized flux spectrum, suggesting a large part of the red peak is not associated with the line-forming region responsible for the double peaks.

A consistency check can be made as to whether the choice of ISP for the correction is reasonable. We have searched the Matthewson et al. (1978) catalogue for field stars nearby the object and found 49 objects within a radius of 180 arcmin (one object with P = 12% was excluded for the analysis). The catalogue also provides photometric estimates of the total extinction A_V to these objects. A relatively tight relation exists between the observed polarization and A_V. A least-squares fit to the data gives the relation P (%) = 1.5 × A_V(mag.) + 0.07. The PA shows mostly a scatter diagram, and gives a mean of 76°± 39° for the total sample. The A_V towards HD 37806 is ambiguous, but likely to be low: Van den Ancker et al. (1998) reclassify HD 37806 as an A2Vpe star and give its extinction as A_V = 0.03. In contrast, Malfait, Bogaert and Waelkens (1998) find an $E(B–V)$ of 0.14 (A_V = 0.43 if the ratio of total to selective reddening, R, is 3.1) for a B9 spectral type. Based on the extinction and the field stars, the ISP towards HD 37806 should be between 0.1% and 0.7%. The 'emission line' method gives 0.36%, a value that is at least consistent with the value returned from the field stars.

Taking the derived intrinsic polarization spectrum at face value, it appears that the Hα line profile is a composite of two unrelated components: a double-peaked polarized component and a single, unpolarized component. Since both the photospheric continuum radiation and the double-peaked component are equally polarized, it would appear that they both appear point-like to the scattering material, while the single component is formed further away
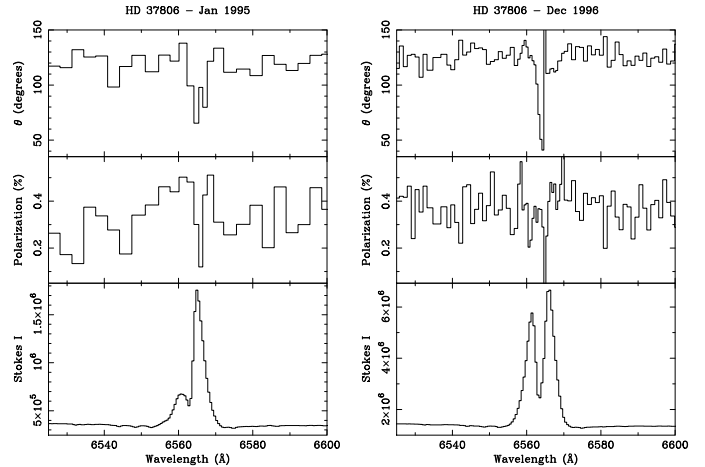

Figure 3. Observed spectra of HD 37806 in 1995 (left hand panel) and 1996 (right hand panel).

from the star, betraying the asymmetry of the scattering region. Perhaps due to the signal-to-noise in the data, no de-polarization is visible in the blue peak. This could suggest that the de-polarization in the red peak is not necessarily due to electron scattering, since one would expect the electron scatterers to be located close to the star. Instead, the data do not exclude the possibility that the red peak is located in an extended nebula (which is not resolved in our data however), while the underlying broader emission and the photosphere are polarized by circumstellar dust, which, by implication, is not distributed spherically symmetric around the star.

Intriguingly, the line-to-continuum ratios of the red peak are constant (see Table 2), while broad-band photometry of this object also appears constant (Van den Ancker et al. 1998) so the blue peak has increased in strength. This fact, combined with the relatively equal red/blue ratio of the double-peaked line in polarized flux, suggests that the polarized red part of the line has also become stronger. This leads to the enigmatic situation that the polarized part of the red peak increased in strength while the unpolarized part of the red peak decreased in strength in such a way that their total has remained constant in time.

Clearly, this object needs further study, both spectropolarimetric, and from a modelling perspective to gain more understanding as to the origin of the observed polarization.

MWC 137 Although Thé et al. (1994) labelled this source as a probable Herbig Be star, in a recent study Esteban & Fernández (1998) argued that is much more likely to be an evolved B[e] supergiant. Their arguments, based on a kinematical association with molecular clouds at more than 5 kpc, are reasonably convincing, but we note that the nature of this source has long been controversial (see references in Esteban & Fernández).

The polarization spectrum and QU diagram of MWC 137 are shown in Fig. 5. The continuum polarization of the object is very large (6%), and slight polarization changes across Hα are visible. Much clearer is the broad, observed rotation of Hα, centered on the line peak. The rotation is
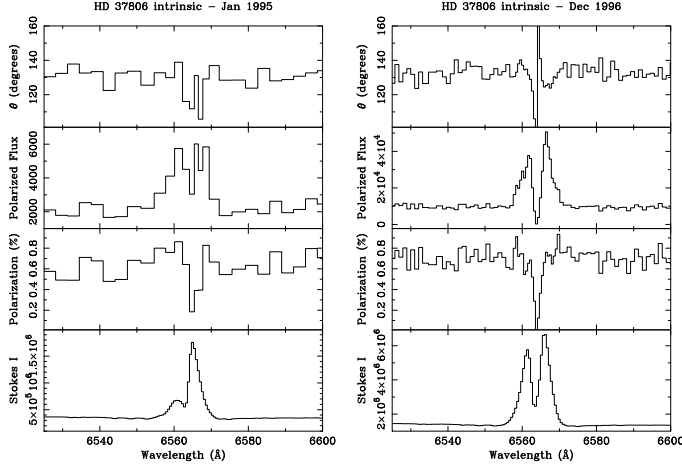
Figure 4. Intrinsic spectra of HD 37806 obtained by assuming the line-center to be intrinsically unpolarized. The second panel shows also the polarized flux (polarization × intensity).
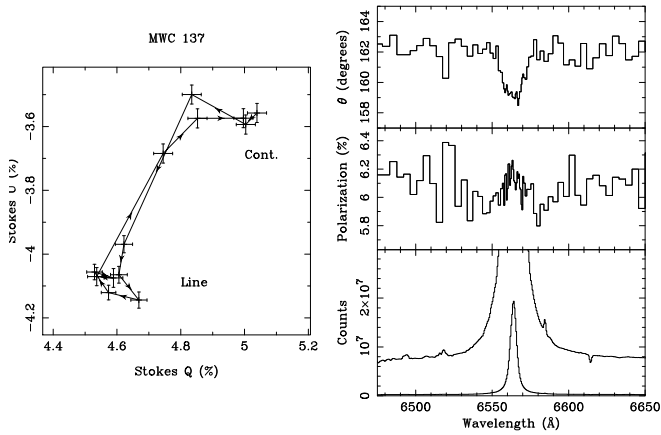

Figure 5. The data on MWC 137. The left panel shows the QU diagram at 0.03% binning, a clear excursion from the continuum is present over the line profile. The right-hand panel shows the polarization spectrum. The intensity is blown up by a factor of 30 for clarity, while the wavelength range is expanded to show the broad line better.

at most only 3°, but it is real as is evident from the significant loop apparent between line and continuum in QU space (Fig. 5); the shift is along the QU vector (+0.3%, +0.5%), corresponding to an intrinsic angle in the continuum of 30° and a depolarization of $\approx 0.6\%$ (measured from the length of the polarization vector, $\sqrt{\Delta Q^2 + \Delta U^2}$). The same situation as for HD 37806 described above occurs in this case: the polarization from intervening material has transformed a de-polarized line into a rotated line. Slight changes in the observed polarization are still present in the wings of the emission, suggesting a different polarization of the line wings than both the continuum or the centre of the emission line.

The interstellar reddening towards the object is very large. It was redetermined by Esteban & Fernández (1998) to be $A_V = 3.77$. This is very high, but according to the au-

thors consistent with a very large distance to the object (the authors mention 6 kpc). If true, then the large continuum polarization can be explained mostly by the interstellar reddening. The polarization of the field stars within a radius of 300′ (taken from Matthewson et al. 1978) increases linearly with A_V up to 4% at $A_V \sim 2.2$, the largest A_V among the field stars in the sample. Unfortunately no information for stars more distant or more reddened is available, but it is clear that a large ISP can be expected for the object.

The rotation across the Hα line is best interpreted as a depolarization across the line, but modified by the intervening ISP and circumstellar dust polarization. Using the 'emission line' method, we find a dust polarization of P=6.2%, Θ=159°, in agreement with the large expected ISP. The intrinsic PA of the electron scattering medium of 30° appears to be parallel with the bright North-Western component of the ring nebula around the object (see again Esteban & Fernández 1998). This may suggest that asymmetries at very small scales, traced by the electron scattering, and at large scales (from the image) are still aligned.

HD 50138 In their search for Herbig Ae/Be stars, Thé et al. (1994) found a subsample of objects with many Herbig characteristics, that nevertheless did not fulfil all their criteria. Based on the strong emission lines, they called this group 'extreme emission line objects'. Most of these stars are also classified as B[e] stars, because of the presence of forbidden lines in the spectrum. HD 50138 is one of these.

Our two observations of HD 50138 (Fig. 6), taken two years apart in January 1995 and January 1997, show essentially the same behaviour. The emission line is double peaked, with a large red to blue ratio of the peaks. The velocity separation of the two peaks is 160 km s^{-1} and the central minimum is at 18 km s^{-1} (helio-centric), which is 15 km s^{-1} blueshifted from the forbidden [O I] line at 6363 Å, for which we measure a central velocity of 33 ± 5 km s^{-1} (helio-centric), in agreement with the radial velocity determination by Pogodin (1997).

The Hα line shows strong de-polarization across the red peak, while the blue peak shows at most a slight depolarization. The 'intrinsic' polarization angle, as deduced from the shift between line and continuum in QU space is about 155°, close to the measured one, implying that the ISP, if any, has had no great effect on the observed polarization characteristics. This is more or less in keeping with the moderate reddening towards this source (van den Ancker et al. 1998 assign $A_V = 0.59$, possibly an upper-limiting value considering that $B - V$ for this mid-B star is close to zero) and the low interstellar polarization in the line of sight, as many objects around HD 50138 have very low polarizations for typical extinction values as 0.5 (Matthewson et al. 1978).

The polarized flux spectrum (polarization × flux, Fig. 6) reveals equally strong blue and red peaks at both epochs. This may indicate that part of the red emission is formed in the same region as the blue peak, such as a rotating disk, but that the excess emission compared to the blue line is formed in a larger volume, resulting in the observed de-polarization. The most straightforward explanation to account for the 'excess' flux in the red peak, as in the case of HD 37806, is that the intensity spectrum is a composite of a rotating disk type of geometry close to the star, and an additional, extended single peaked component.
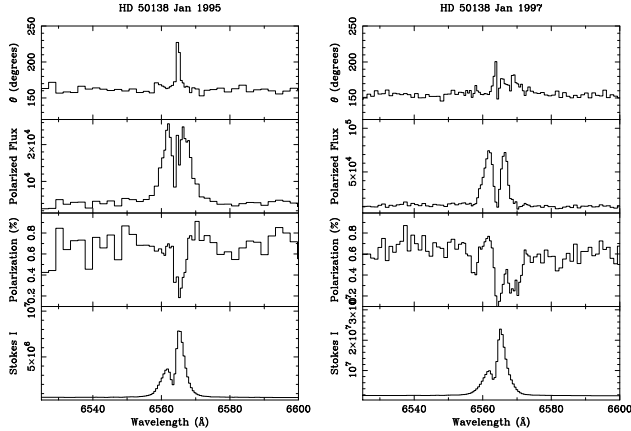
Figure 6. The polarization data on HD 50138 in 1995 and 1997 respectively, the polarized flux is also plotted.

A clue to the line formation may be provided by the spectrum taken around the lower opacity Hβ line by Jaschek & Andrillat (1998). Their published Hβ profile shows the blue and red peaks roughly equal, with some underlying photospheric absorption still visible. The much larger red-to-blue ratio in Hα could imply that the excess red emission in Hα is optically thin - since for thin HI emitting gas the Balmer decrement may be substantially steeper than for optically-thick gas. The double-peaked part of the line could then be an optically-thick line formed very close to the star, while the unpolarized line is optically-thin.

It is clear that any picture of this object must be simplified since the spectrum of HD 50138 shows many more peculiarities. Grady et al. (1996) include this star in their sample of objects exhibiting β Pic type infall phenomena. Pogodin (1997) drew attention to the variable HeI λ5876 line profile, which sometimes shows an inverse P Cygni behaviour. He also attributed this to infall of material.

HD 87643 HD 87643 is a B[e] star, for which evidence suggests that it is located at several kpc, indicating a massive and evolved nature of the object. This, and its spectroscopic and spectropolarimetric data have been analysed in more detail in Oudmaijer et al. (1998). For completeness we show the data and the spectrum corrected for ISP and circumstellar polarization in Fig. 7. The polarization of this object shows some striking features. After correction for the intervening polarization, it turns out that most of this structure appears an artefact due to the polarization vector additions; the spectrum corrected for ISP and circumstellar dust has a much smoother behaviour. A comparison with the schematic model calculations by Wood, Brown & Fox (1993) indicates that the polarization profile can be best reproduced with a circumstellar disk that is both rotating and expanding.

HD 45677 From their UV - optical low resolution spectropolarimetry Schulte-Ladbeck et al. (1992) infer that HD 45677 is surrounded by a bipolar nebula. After correcting for ISP, the polarization angle of the blue/UV spectrum they present is rotated by about 90° with respect to the red part of the spectrum. The explanation advanced for this behaviour is that the red emission is scattered through a dust
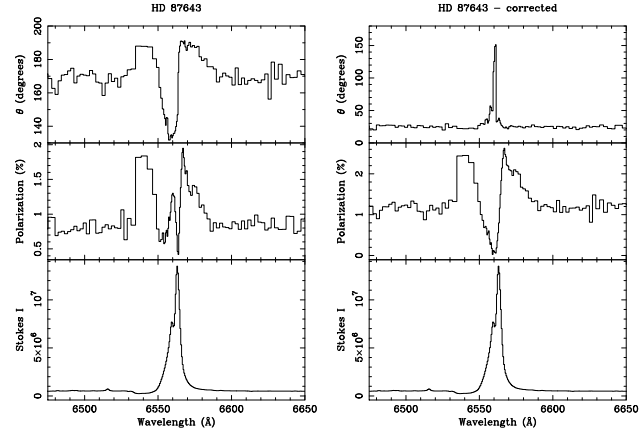

Figure 7. The polarization spectrum of HD 87643, and the corrected spectrum of the star. The wavelength range is expanded to show the broad line better. For more details, see Oudmaijer et al. (1998).
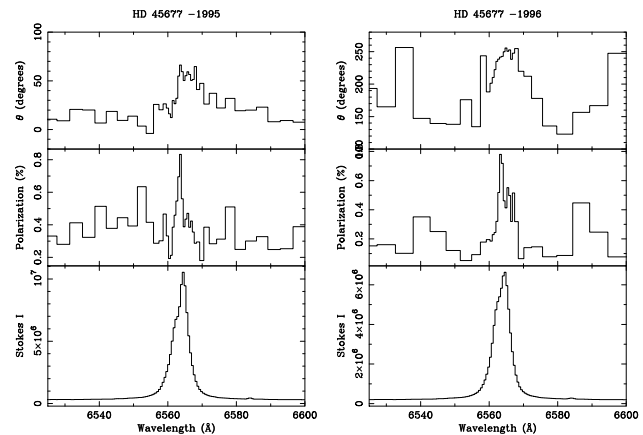

Figure 8. The polarization spectrum of HD 45677 in 1995 and 1996.

torus, while the blue emission, to which the dust is optically thick, comes from a scattering bipolar flow, perpendicularly oriented with respect to the torus.

The spectra taken in January 1995 and December 1996 are shown in Fig. 8. On both occasions the polarization across Hα is enhanced with respect to the continuum. The variability of the continuum polarization is very strong, with the polarization changing from 0.4% to 0.2%, while the position angle changed from 11° to 140°. The peak of Hα shows in both cases roughly the same polarization and position angle ($\sim$0.8%, 75°). Although Hα is enhanced in the observed polarization spectrum, this does not necessarily imply that the intrinsic spectrum exhibits the same effect. In the following we discuss the different elements, ISP, circumstellar dust scattering and electron-scattering that shape the observed polarization spectra. As explained below, we assume that the polarization changes across Hα are due to electron-scattering.

The spectra are plotted in QU space in Fig. 9. Both circumstellar dust polarization and ISP add only a constant

QU vector to all points. The continuum points cluster at different positions on the dates of observation, while the QU vectors across Hα are almost parallel. A least squares fit through the QU-points between 6550 and 6570 Å, returns intrinsic polarization angles of $168 \pm 3°$ and $163 \pm 3°$ for the 1995 and 1996 spectra respectively. Depending on the quadrant where the intrinsic QU vectors are located, these values could be rotated by $90°$ and define a projected angle on the sky of $\approx 75°$. The length of the vector on both occasions corresponds to $P \approx 0.95\%$, assuming the line to be unpolarized. The electron-scattering region is thus aspherical, has a PA of $\sim 75°$ on the sky at a relatively constant amplitude of about 0.95% .

How does this relate to the view taken by Schulte-Ladbeck et al. (1992) of their similar detection of enhanced Hα linear polarization? In their ISP-corrected spectrum, Hα is still enhanced with respect to its adjacent continuum. They explained this in terms of an ionized region much closer to the circumstellar dust than the stellar point source: the Hα line then sees a larger solid angle of scattering material and is thus more polarized than the continuum. This seems to us an unlikely alternative to the conventional view that the ionized region, with a temperature of $\sim$10000 K, is located within a very much smaller volume around the star than the dust, which should have an equilibrium temperature below $\sim$1500 K, the dust condensation temperature (see e.g. the spectral energy distribution modelling of HD 45677 by Sorrell 1989). Furthermore, the ISP correction adopted by Schulte-Ladbeck et al. (1992) was the *ad hoc* value proposed by Coyne & Vrba (1976) on the basis that it should be comparable with the relatively steady observed polarization in the blue (the red is much more variable). Whatever this correction actually does correspond to, there is no reason to suppose that it accounts for both the ISP and circumstellar dust polarization. If both sources of foreground polarization can be removed with confidence, only then can it be discerned whether there is an intrinsic linear polarization enhancement across Hα. Hence, for the timebeing, we retain the more conventional view that the observed polarization change across Hα is due to electron scattering in the ionized region, which may project as an oblate 'disk' or as a prolate 'bipolar flow'.

Now we turn to consider the change in polarization of the continuum points. As it is likely that the ISP is constant in time, the additional, potentially variable, mechanisms involved are electron-scattering and circumstellar dust scattering. In the same manner as the polarization changes across Hα move along a constant angle, temporal changes, due to a polarization mechanism that becomes stronger or weaker, may only affect the magnitude of polarization and not the PA. If we adopt this principle here, the intrinsic PA of the polarizing material responsible for the change in continuum polarization is then $\sim 20°$.

Since the intrinsic PA of the electron scattering region is $\sim 75°$, and its effect on the Hα line appears not to have changed significantly, the variable component does not seem to be electron scattering. This leaves circumstellar dust scattering as the likely variable. Although the polarization variability of HD 45677 is well known, dating back to the paper in 1976 by Coyne & Vrba, it is only the high spectral resolution of the current data that allows us to discriminate between electron and dust scattering.
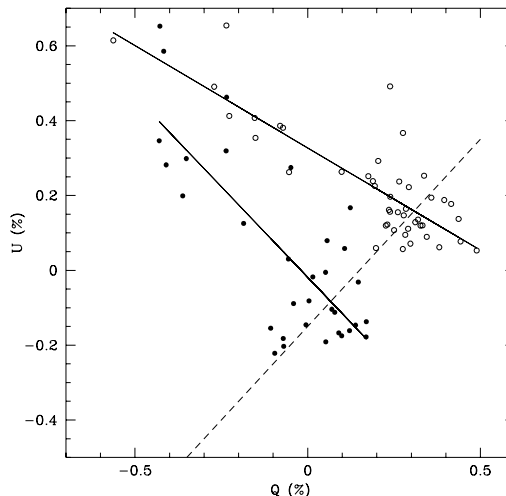

Figure 9. QU data of HD 45677 of both epochs at 0.04% binning. Open circles represent the January 1995 data, and filled circles the December 1996 data. The solid lines are fits through the line data, and the dashed line represents a fit through the two continuum points.

The major question remaining is why the apparent rotation of about $55°$ between the major axis of the (variable) dust polarization and the Hα line forming region exists. In principle, this would suggest that multiple geometries, such as a combination of an equatorial disk and a bipolar flow, would show a rotation of $90°$, regardless of the respective opening angles. The cancellation of perpendicularly-oriented polarization vectors tends to increase for larger opening angles, decreasing the observed polarization percentage, but the $90°$ rotation will remain intact. An answer may lie in the clumpiness of the dusty material around the object. HD 45677 is photometrically variable, a property attributed to the presence of various dust-clouds surrounding and even orbiting the object (de Winter & van den Ancker 1997). Clumpy material is also revealed by the spectroscopic variability. Grady et al. (1993) show the presence of variable redshifted absorption lines which are attributed to infalling and evaporating cometary bodies. These indicate patchiness of the circumstellar material as well.

The result of such clumpy material on the polarization angle is relatively easy to understand. If (one of) the scattering regions is clumpy, a rotation of $90°$ is only retrieved if the clumps are symmetrically distributed around the central star. If not, not all perpendicularly oriented polarization vectors will cancel out, and the net effect is that the observed position angle does not represent the time-averaged mean orientation of the scattering material. A similar argument has been brought forward by Trammell et al. (1994) to explain the rotation of $70°$ (instead of $90°$) in the spectrum of IRAS 08005-2356. It seems thus that the rotation between the dust ring and the Hα line forming region, which is less than $90°$, could be the result of scattering with incomplete cancellation in an inhomogeneous region.

A word of caution should be given here with regard to the 'true' orientation of the dusty material. The $20°$ that was measured between the continuum points in Fig. 9, and its

comparison with the intrinsic angle of the electron scattering region points to the clumpiness. However, this direction along which the variation occurred should not now be associated with the orientation of the scattering region, since we only measure incomplete cancellation of dust clumps at changing positions. Only sequences of observations of this type may give a clue as to whether the variable dust component arises from a region perpendicular to or colinear with the electron scattering region.

The main result of the new observations of HD 45677 is that it is possible to discriminate between the *electron* scattering and the *dust* scattering regions. The former can be probed by the change across Hα while the latter is probed by the variability of the polarization of the continuum.

4   DISCUSSION

4.1   What the observations tell us

This paper concerned medium resolution spectropolarimetry of a relatively large sample of B[e] and Herbig Be stars, objects which so far have never been observed in this way. We have described the results of these exploratory observations in a qualitative way and we summarize the highlights of both non-detections and detections below, and then briefly discuss the implications of the results.

4.1.1   'Non'-detections

The main goal of the observations was to answer the basic question "Does the ionized material around these stars project to circular symmetry on the sky, or not?" by investigating whether or not a 'line-effect' is seen across Hα. In principle, a non-detection should imply a circular projection. This encompasses three-dimensional geometries that are spherically-symmetric, or disk-like seen close to face-on.

Two of the non-detections failed in quite different ways to fit into this simple picture:

First, in the case of MWC 297 – a young B1.5 star in the Aquila Rift (Drew et al. 1997) – observation over two hours or so produced evidence of, at most, a subtle line effect. This was despite the fact that the radio image of this object shows a clearly elongated ionized gas distribution. An intriguing interpretation, testable by high resolution imaging, is that we view MWC 297 only indirectly at optical wavelengths. If the direct sightline to the disk should reveal an edge-on structure, but if the disk is obscured from view due to the large extinction, scattering dust clouds may see a more circularly symmetric structure, such as a face-on disk, and reflect a polarization spectrum without a line effect to the observer.

Second, we have presented data on ω Ori, a star that has been reported twice before in the literature as showing an Hα line effect (in both instances the observations were narrow-band rather than spectropolarimetric). The absence of any such effect in our data suggests that the ionized envelope is smaller than at previous occasions because the, optically thin, electron-scattering is more sensitive to changes in ionization than the optically thick Hα emission. The non-detection in ω Ori implies that single epoch measurements

are not always sufficient to provide a definitive answer on the circumstellar geometry of these objects.

In both cases, it is clear that Hα spectropolarimetry is best judged in the context of other observational constraints on the target. Indeed they warn not to assume *too* quickly that the ionized regions in stars without a line effect are face-on disks or spherically-symmetric.

4.1.2   Objects displaying a line-effect

In contrast, the detection of a line-effect immediately tells us that the scattering region does not project to circular symmetry on the sky. The data presented in this paper provide a new, richer variety of line effects than has hitherto been seen in the literature. This is in part due to their relatively high spectral resolution.

The curious cases of the somewhat similar situations of HD 37806 and HD 50138 offer great opportunities to understand the conditions close to the star. Both objects show double peaked Hα line profiles, that have different V/R ratios in normal intensity spectra, but which turn out to be of equal strength in the polarized flux data. Both stars also exhibit a superposed single component of Hα emission that is also picked out by a change in linear polarization at much the same wavelength. This suggests that the line profile as a whole may be the result of two kinematically-distinct phenomena. These may be a rotating disk (or self-absorbed compact nebula), and a spatially more extended region of less-rapidly expanding HII whose emission is only polarized by the ISM.

A particularly striking result to emerge from our data concerns the probable Herbig Be star, HD 53367. We have observed depolarization across Hα without angle rotation. The co-alignment of the local interstellar magnetic field and stellar rotation axis together with the findings of Vrba et al. (1987), favour formation of this relatively massive star ($M > 10 \, M_\odot$) by collapse rather than by the merger of less massive stars.

The power of repeated observations is shown by the case of HD 45677. Due to the continuum variability and the constant polarization arising from electron scattering, it is possible to distinguish between the electron and circumstellar dust scattering mechanisms. This is the first time that it has been possible to do this. Since the measured intrinsic angles of the dusty and the ionized region differ by 55° rather than 90° (for perpendicular geometries) or 0° (for parallel geometries) we can conclude that the the dust component is clumpy.

4.2   Implications for Herbig Be and B[e] star research

Among the probable Herbig Be stars we have observed, around half of them have shown no detectable line effect (LkHα 218, HD 52721, V380 Ori and MWC 297). This of course means that almost half have (namely HD 259431, HD 37806 and HD 53367) and should encourage further campaigns of this nature. Using narrow bands, Poeckert & Marlborough (1976) surveyed 48 Be stars and found that 21 showed the line effect at a 3σ level, while a further 8 show the line effect at a 2-3σ level. They investigated the relation between the intrinsic polarization of these Be stars (measured

from the Hα polarization change) with $v \sin i$ (as measure of inclination) and found that their observations could well be explained by inclination effects. Although based on very small number statistics, the comparable incidence of line effects in the Herbig Be stars observed does hint that flattened ionized circumstellar structures are quite common for this object class as well, and that the non-detections in our sample could be due to random sampling of the full range of inclinations. One of our non-detections is of course MWC 297, an object revealed by radio imaging to be non-circular (albeit on a scale of tens of AU).

It is important to appreciate that the Hα polarization effect is sensitive to much smaller structures than are presently probed directly by imaging. Analytical calculations such as those by by Cassinelli, Nordsieck & Murison (1987, their Fig. 7) demonstrate that the bulk of electron scattering occurs on scales as small as two to three stellar radii. If the Herbig Be stars we have observed are indeed young or even pre-main sequence objects, then the deviation from spherical symmetry of the ionized region is presumably a consequence of the way in which they have formed. Viewed in these terms, the structures that we detect now via these polarization measurements could well be accretion disks that reach to within a stellar radius or so of the stellar surface. This conclusion is at variance with the magnetospheric accretion model widely regarded as applicable to T Tau stars, wherein magnetic channeling inhibits the formation of the inner disk (see Shu et al. 1994). For Herbig Be stars it remains a more open question as to how far magnetic fields determine the accretion geometry. Since the main sequence destiny of these more massive stars is to possess radiative envelopes, it leaves more room to doubt that magnetic fields must play a big role at the stage in which we are able to observe them. It will be interesting to see if further Hα spectropolarimetry continues to uncover plausible disk accretors.

A conceptual model of how these objects may look, still embedded in accretion disks reaching into the stellar surface, has recently been devised by Drew, Proga & Stone (1998, building on the work of Proga, Stone & Drew 1998). This work shows how observationally-significant disk winds, driven by radiation pressure, would be created. A further piece in the puzzle of Herbig Be and BN objects that these predicted flows can help explain is the high contrast, quite narrow HI line emission often observed at earlier B spectral types (Drew, 1998).

A further very strong outcome of this study is that all objects that can be classified as (evolved) B[e] stars, presented significant polarization changes across Hα. A factor that clearly helps increase the likelihood of detecting a spectropolarimetric line effect in B[e] stars is that their Hα profiles are typically extremely high contrast and often somewhat broader than in Herbig Be stars. Pre-eminent among our B[e] group is HD 87643 which has already been discussed in a separate paper (Oudmaijer et al. 1998). Here we have presented MWC 137 (probably an evolved B[e] star), HD 45677 and HD 50138. The fact that *all* observed Galactic B[e] stars in our sample show the line-effect in one incarnation or another lends strong support to the Zickgraf et al. (1985, 1986) model. The variety of line-effects observed in our data illustrate that the structures around these stars have their deviation from spherical symmetry in common,

but that the details in each case are different. So far, the discussion of these data has been largely qualitative. As models simulating these phenomena begin to be calculated there will no doubt be a considerable sharpening of insight.

5 FINAL REMARKS

Apart from providing some striking insights into a number of the targets observed, the programme of observations we have described here has offered some lessons in how best to obtain single-line spectropolarimetric data. It is clear that the spectral resolution available to us ($R \approx 5000$) has in most instances been just enough. As numerical modelling becomes more commonplace, the case for increased spectral resolution will become stronger. The main issue, nevertheless, is the achievement of high enough data quality. Our 8th magnitude and brighter objects have come out well in under an hour's telescope time, while 10th to 12th magnitude objects require several hours observation with a 4-metre class telescope in at least middling weather conditions. Ultimately, these fainter sources will be best served by 8-metre class facilities where the shorter total integration times will be less subject to weather influence – presently they can be an uncertain struggle.

The overall conclusion of this study is that this relatively unexplored mode of observing does yield valuable new insights. In some instances we have encountered deepening mysteries that suggest conclusions drawn from other data have missed something. MWC 297 and HD 45677 are both good examples of this. At the same time, Hα spectropolarimetry readily throws up examples that demand sophisticated numerical modelling of a type that is just beginning to become available (Hillier, 1996; Harries, 1996).

REFERENCES

Allen D.A., Swings J.P. 1976, A&A 47, 293
Bergner Yu.K. et al 1988, Afz 28, 529
Blommaert J.A.D.L., van der Veen W.E.C.J., Habing H.J. 1993, A&A 267, 39
Bonnell I.A., Bate M.R., Zinnecker H. 1998, MNRAS 298, 93
Burrows C.J. et al. 1996, ApJ 473, 437
Cassinelli J.P., Nordsieck K.H., Murison M.A. 1987, ApJ 317, 290
Clampin M., Schulte-Ladbeck R.E., Nota A., Robberto M., Paresce, Clayton G.C. 1995, AJ 110, 251
Claria J.J. 1974, A&A 37, 229

Clarke D., McLean I.S. 1974, MNRAS 167, 27

Clarke D., Brooks A. 1984, MNRAS 211, 737

Corcoran M., Ray T.P. 1997 A&A 321, 189

Coyne G.V. & Vrba F.J. 1976, ApJ 207, 790

de Winter D., van den Ancker M.E. 1997, A&AS 121, 275

Drew J.E. 1998, in ASP Conf. Series 131 *Boulder-Munich II: Properties of hot, luminous stars*, ed. I.D. Howarth, Astron. Soc. Pac., San Francisco, p. 14

Drew J.E., Busfield G., Hoare M.G., Murdoch K.A., Nixon C.A., Oudmaijer R.D. 1997, MNRAS 286, 538

Drew J.E., Proga D., Stone J.M. 1998, MNRAS 296, L6

ESA, "The Hipparcos and Tycho Catalogues", 1997, ESA SP-1200

Esteban C., Fernández M. 1998, MNRAS 298, 185

Finkenzeller U. 1985, A&A 151, 34

Frank A. and Mellema G. 1996, ApJ 472, 684

Gnedin IU. N., Kiselev N.N., Pogodin M.A., Rozenbush A.E., Rozenbush V.K. 1992, AZhL 18, 454

Grady C.A., Pérez M.R., Talavera A. et al. 1996, A&AS 120, 157

Grady C.A., Bjorkman K.S., Shepherd D., Schulte-Ladbeck R.E., Perez M.R. 1993, ApJ 415, L39

Grinin V.P. et al. 1994, A&A 292, 165

Gummersbach C.A., Zickgraf F.-J., Wolf B. 1995, A&A 302, 409

Harries T.J. 1996, A&A 315, 499

Herbig G.H. 1960, ApJS 4, 337

Herbig G.H., 1994, in ASP Conf.Sers. No. 62 *The Nature and evolutionary status of Herbig Ae/Be stars*, eds. P.S. Thé , M.R. Pérez, E.P.J. van den Heuvel, Astron. Soc. Pac., San Francisco p. 3

Herbst W., Racine R., Warner J.W. 1978, ApJ 223, 471

Herbst W., Warner J.W., Miller D.P., Herzog A. 1982, AJ 87, 98

Hillenbrand L.A., Strom S.E., Vrba F.J., Keene J. 1992, ApJ 397, 613

Hillier D.J. 1996, A&A 308, 521

Hoare M.G., Garrington S.T. 1995, ApJ 449, 874

Jain S.K. Bhatt H.C. 1995, A&AS 111, 399

Jaschek C., Andrillat Y. 1998, A&AS 128, 475

Magalhães A.A. 1992, ApJ 398, 286

Malfait K., Bogaert E., Waelkens C. 1998, A&A 331, 211

Mannings V., Koerner D.W., Sargent A.I. 1997, Nat. 388, 555

Matthewson D.S., Ford V.I., Klare G., Neckel T., Krautter J. 1978, *Bull. Inf. CDS*, 14, 115

McLean I.S., Clarke D. 1979, MNRAS 186, 245

Miller W.C., Merrill P.W. 1951, ApJ 113, 624

Miroshnichenko A.S., Ivezić Ž, Elitzur M. 1997, ApJ 475, L41

Osterbart R., Langer N., Weigelt G. 1997, A&A 325, 609

Oudmaijer R.D., Drew J.E. 1997, A&A 318, 198

Oudmaijer R.D., Proga D., Drew J.E., de Winter D. 1998, MNRAS 300, 170

Pezzuto S., Strafella F., Lorenzetti D. 1997, ApJ 485, 290

Poeckert R. 1975, ApJ 152, 181

Poeckert R., Marlborough J.M. 1976, ApJ 206, 182 (PM)

Pogodin M.A. 1997, A&A 317, 185

Proga D., Stone J.M., Drew J.E. 1998, MNRAS 295, 595

Schmidt-Kaler Th. 1982, in Landolt-Börnstein, Numerical Data and Functional Relationships in Science and Technology, New Series Group VI, Vol. 2b, Springer-Verlag

Schulte-Ladbeck R.E., Shepherd D.S., Nordsieck K.H. et al. 1992, ApJ 401, L105

Schulte-Ladbeck R.E., Clayton G.C., Hillier D.J., Harries T.J., Howarth I.A. 1994, ApJ 429, 846

Shu F., Najita J., Ostriker E., Wilkin F., Ruden S., Lizano S. 1994, ApJ 429, 781

Slettebak A. 1988, PASP 100, 770

Sonneborn G. et al. 1988, ApJ 325, 784

Sorrell W.H. 1989, MNRAS 241, 89

Stenholm B. Acker A. 1987, A&AS 68, 51

Thé P.S., de Winter D., Perez M.R. 1994, A&AS 104, 315

Tinbergen J., Rutten R. 1997, 'Measuring polarization with ISIS'

Tody D. 1993, in ASP Conf. Series 52 *Astronomical Data Analysis Software and Systems II*, eds. R.J. Hanisch, R.J.V. Brissenden, J. Barnes, Astron. Soc. Pac., San Francisco, p. 173.

Trammell S.R., Dinerstein H.L., Goodrich R.W. 1994, AJ 108, 984

van den Ancker M.E., de Winter D., Tjin a Djie H.R.E. 1998, A&A 330, 145

Vrba F.J., Baierlein R., Herbst W. 1987, ApJ 312, 207

Waelkens C., Van Winckel H., Waters L.B.F.M., Bakker E.J. 1996, A&A 314, L17

Welsh B.Y. 1991, ApJ 373, 556

Wood K., Brown J.C., Fox G.K. 1993, A&A 271, 492

Zickgraf F.-J., Schulte-Ladbeck R.E. 1989, A&A 214, 274

Zickgraf F.-J., Wolf B., Stahl O., Leitherer C., Klare G. 1985, A&A 143, 421

Zickgraf F.-J., Wolf B., Stahl O., Leitherer C., Appenzeller I. 1986, A&A 163, 119